Correlation diagrams for rigid and nonrigid five-body and XY_5 six-body systems

Gregory S. Ezra and R.Stephen Berry

Department of Chemistry and the James Franck Institute, The University of Chicago, Chicago, Illinois 60637
(Received 5 November 1980; accepted 22 June 1981)

Correlation diagrams are constructed to connect the rotation–vibration energy levels of idealized limiting models for penta-atomic molecules. One limit is the completely nonrigid homonuclear five-body cluster. The method of plethysms is applied to classify the states of the nonrigid limit.Several rigid limits are considered: trigonal bipyramidal, tetrahedral, square pyramidal, pentagonal planar, and regular linear chain molecules. The tetrahedral and square pyramidal examples are generalized to allow the atom in the unique central position to differ from the rest giving (four + one)-body systems. A rigid/nonrigid energy level correlation diagram is also constructed for an XY_5 molecule having trigonal bipyramidal point symmetry in the rigid limit. The steps are outlined that will be necessary for applying these diagrams to the interpretation of real molecular spectra.

I. INTRODUCTION

The classification of vibration–rotation states of molecules exhibiting an arbitrary degree of nonrigidity has been the goal of a recent line of research of which this work is a part.[1–3] We seek ways to assign quantum numbers to states and transitions, to compute approximate density-of-states functions, and to infer the nature and extent of the nonrigidity of a molecule from its rovibronic spectrum. Moreover, we require that this method be free of the limitations inherent in a perturbation-theoretic treatment of nonrigidity.[4,5]

Our approach has been to consider two idealized limiting cases: (1) a rigid molecule with small amplitude vibrations and rigid-body rotations, in which there is negligible rotation–vibration interaction, and (2) a completely nonrigid collection of particles interacting via pairwise attractive harmonic forces, for which there is complete mixing of vibrations with rotations. The appropriate energy level sequences for these model systems are easily constructed and the quantum numbers and degeneracies of the levels are equally easily determined. The quantum numbers of the limiting cases characterize constants of the motion of the idealized extremes, but do not correspond to exactly conserved quantities in real systems. When the idealized limits are connected, we obtain energy level correlation diagrams. The connection is accomplished by classifying all states according to the kinematic symmetry quantum numbers assumed valid throughout, i.e., total angular momentum, parity and character with respect to permutation of identical particles, and invoking the noncrossing rule.

We emphasize that for a given molecule we are considering two model Hamiltonians whose dynamical symmetries correspond to approximate constants of the motion near the limiting cases. A useful analogy can be made here with Mulliken's united-atom separated-atom correlation diagrams for homonuclear diatomics. As is well known, one-electron states of the united-atom limit have extra degeneracies due to the O(4) dynamical symmetries of hydrogenic systems; this corresponds to the high dynamical symmetry of our nonrigid oscillator limit. Moreover, the separated-atom limit also has nontrivial degeneracies of g and u states which are analogous to structural degeneracies[6] of rigid molecule states in our idealized rigid limit. The group theory describing "accidental" structural degeneracies has been investigated by Natanson.[7]

In previous studies, energy level correlation diagrams were constructed for the three-body[1,3] and four-body problem,[2] including several rigid or semirigid limiting cases. The example that perhaps brought us closest to real spectroscopy was the $(H_2)_2$ molecule, which has been the subject of several recent experimental and theoretical investigations.[8]

In this work, we extend the construction of idealized correlation diagrams to the case of five identical particles, and to the case of polyhedral XY_n molecules with four and five identical Y atoms around a central X atom. These last examples bring us closer still to the analysis of actual spectra.

The present work has two main goals: first, we apply the general and efficient method of plethysms to generate the correlation diagrams for systems containing five and six particles. Second, we wish to lay the groundwork for interpreting spectroscopic studies at the resolution of saturation spectroscopy[9] of vibrationally excited nonrigid species such as PF_5.

In our view, the present work carries the construction of rigid/nonrigid correlation diagrams for simplified model systems as far as can be justified for its own sake. With this paper, we complete the development of tools for constructing correlation diagrams as required. Future work will develop the application of these diagrams as classification devices for real spectra, and address the problem of intensities in nonrigid molecule spectra.

In the next section the idealized models for the nonrigid and rigid limits are briefly reviewed. The states of the nonrigid five-particle and (four + one)-particle (one particle distinct) systems are classified according to their kinematic symmetries using the method of *inner plethysms*.[10–14] This method is significantly more ef-

 0021-9606/82/073679-13$02.10

ficient than elementary methods, especially for complex molecules. Five distinct rigid structures are then considered: pentagonal ring (D_{5h}), linear ($D_{\infty h}$), trigonal bipyramid (D_{3h}), tetrahedral (T_d), and square pyramidal (C_{4v}). The last two cases are generalized to allow the particle in the unique central position to differ from the others, so that we can also describe methane-like molecules and square pyramidal XY_4 molecules. The rigid/nonrigid energy level correlation diagrams for the five-body problem are presented in Sec. III. In Sec. IV we apply our method to the construction of a correlation diagram for an XY_5 molecule whose rigid limit is a trigonal bipyramid with D_{3h} symmetry. We conclude with an explicit enumeration of the steps to connect these diagrams with the level schemes of real molecules where some of the idealized symmetry is broken.

II. THE FIVE-BODY PROBLEM: IDEALIZED LIMITS

A. Nonrigid limit

As previously, the nonrigid limit is here taken to be a cohesive assembly of identical particles (nuclei) held together by pairwise attractive harmonic forces. We suppose that, in the nonrigid limiting case, the molecule has so much "empty space" that virtually all pairwise encounters occur at impact parameters greater than the hardcore repulsion radius of the particles. This in turn means that we can take the equilibrium distance for the pairwise forces to be effectively zero. Such an extreme example of a nonrigid system is well known in nuclear physics,[15,16] but has not commonly been used as a model for molecules or clusters. Indeed, it is not necessarily a particularly realistic limit, but, like the equally idealized united-atom limit for diatomic molecules, it is important because it offers a well-understood terminus for energy levels. The nonrigid limit provides a well-defined sequence of energy levels, degeneracies, and decomposition of degenerate sets of states according to physically significant quantum numbers.

When expressed in suitable Jacobi coordinates, the Hamiltonian for the nonrigid limit separates into the translational kinetic energy of the center of mass $\mathcal{H}_{\rm com}$ and an internal Hamiltonian $\mathcal{H}_{\rm int}$ describing $3N-3$ ($=12$ for $N=5$) independent identical harmonic oscillators[16]:

$$\mathcal{H}=\mathcal{H}_{\rm com}+\mathcal{H}_{\rm int}\ . \tag{1}$$

The Hamiltonian $\mathcal{H}_{\rm int}$ is invariant with respect to all unitary transformations among the 12 oscillator degrees of freedom, so that the symmetry group of the harmonic system is the unitary group U(12).[17] The degenerate states of the nonrigid limit therefore span irreducible representations (IRs) of U(12); in particular, the totally symmetric IRs corresponding to zero, one, two and successively higher numbers of bosons (quanta), which for ν quanta are specified by a Young pattern $[\nu]$ consisting of a single row of ν boxes.[18] The degeneracy of the totally symmetric IR $[\nu]$ of U(12) corresponding to ν quanta is

$$g_\nu=\frac{(n+\nu-1)!}{\nu!\,(n-1)!} \tag{2}$$

TABLE I. Classification of five-body nonrigid states according to their parity, angular momentum and permutation symmetry. Components of the row vectors give the number of IRs [5], [41], [32], [31^2], [2^21], [21^3], and [1^5] of S_5, respectively.

ν	π	g_ν	$J=0$	1	2	3	4	5	6
0	+	1	(1,0,0,0,0,0,0)						
1	−	12		(0,1,0,0,0,0,0)					
2	+	78	(1,1,1,0,0,0,0)	(0,0,0,1,0,0,0)	(1,1,1,0,0,0,0)				
3	−	364	(0,0,0,0,0,1,0)	(1,3,2,2,1,0,0)	(0,1,1,1,1,0,0)	(1,2,1,1,0,0,0)			
4	+	1365	(3,4,4,1,2,0,0)	(0,2,2,4,2,2,0)	(3,6,6,4,3,1,0)	(0,2,2,3,1,1,0)	(2,3,2,1,1,0,0)		
5	−	4368	(0,0,1,2,2,2,1)	(4,12,11,11,7,3,0)	(2,7,8,9,7,5,1)	(4,11,10,10,6,3,0)	(1,4,4,4,3,2,0)	(2,4,3,3,1,0,0)	
6	+	12376	(7,13,13,8,7,3,1)	(1,11,12,19,12,11,1)	(10,26,28,24,20,10,2)	(4,15,16,21,14,11,2)	(7,18,18,16,12,6,1)	(1,6,6,8,5,3,0)	(3,6,5,3,2,1,0)

TABLE II. Classification of (four + one)-body nonrigid states according to their parity, angular momentum and permutation symmetry. Components of the row vectors give the number of IRs [4], [31], [2^2], [12^2], and [1^4] of S_4, respectively.

$U(9)\ U(3)$								
$\nu\ \nu'$	π	$j=0$	1	2	3	4	5	6
(0,0)	+	(1,0,0,0,0)						
(1,0)	−		(0,1,0,0,0)					
(0,1)	−		(1,0,0,0,0)					
(2,0)	+	(1,1,1,0,0)	(0,0,0,1,0)	(1,1,1,0,0)				
(1,1)	+	(0,1,0,0,0)	(0,1,0,0,0)	(0,1,0,0,0)				
(0,2)	+	(1,0,0,0,0)		(1,0,0,0,0)				
(3,0)	−	(0,0,0,0,1)	(1,3,1,2,0)	(0,1,1,1,0)	(1,2,0,1,0)			
(2,1)	−	(0,0,0,1,0)	(2,2,2,1,0)	(1,1,1,1,0)	(1,1,1,0,0)			
(1,2)	−		(0,2,0,0,0)	(0,1,0,0,0)	(0,1,0,0,0)			
(0,3)	−		(1,0,0,0,0)		(1,0,0,0,0)			
(4,0)	+	(3,3,3,1,0)	(0,2,1,3,1)	(3,5,4,3,1)	(0,2,1,2,1)	(2,2,2,1,0)		
(3,1)	+	(1,3,1,2,0)	(1,4,2,3,1)	(2,6,2,4,0)	(1,3,1,2,0)	(1,2,0,1,0)		
(2,2)	+	(2,2,2,0,0)	(1,1,1,2,0)	(3,3,3,1,0)	(1,1,1,1,0)	(1,1,1,0,0)		
(1,3)	+	(0,1,0,0,0)	(0,1,0,0,0)	(0,2,0,0,0)	(0,1,0,0,0)	(0,1,0,0,0)		
(0,4)	+	(1,0,0,0,0)		(1,0,0,0,0)		(1,0,0,0,0)		
(5,0)	−	(0,0,1,1,1)	(3,10,4,7,1)	(2,5,4,6,2)	(3,9,4,7,1)	(1,3,2,3,1)	(1,4,1,2,0)	
(4,1)	−	(0,2,1,3,1)	(6,10,8,7,2)	(3,9,6,8,3)	(5,9,7,6,2)	(2,4,3,3,1)	(2,2,2,1,0)	
(3,2)	−	(0,1,1,1,1)	(3,9,3,6,0)	(2,7,3,5,1)	(3,8,2,5,0)	(1,3,1,2,0)	(1,2,0,1,0)	
(2,3)	−	(0,0,0,1,0)	(3,3,3,1,0)	(2,2,2,2,0)	(3,3,3,1,0)	(1,1,1,1,0)	(1,1,1,0,0)	
(1,4)	−		(0,2,0,0,0)	(0,1,0,0,0)	(0,2,0,0,0)	(0,1,0,0,0)	(0,1,0,0,0)	
(0,5)	−		(1,0,0,0,0)		(1,0,0,0,0)		(1,0,0,0,0)	
(6,0)	+	(6,8,6,4,2)	(1,7,4,10,3)	(8,17,13,12,4)	(3,10,6,11,4)	(6,12,9,9,3)	(1,4,3,5,1)	(3,4,3,2,1)
(5,1)	+	(3,10,4,7,1)	(5,15,9,14,4)	(8,24,12,20,4)	(6,17,10,16,4)	(5,16,7,12,2)	(2,7,3,5,1)	(1,4,1,2,0)

with $n=12$. The levels of the 12-dimensional oscillator are of course equally spaced, with an interval $\hbar\omega=(5k/m)^{1/2}$, where k is the interparticle force constant and m is the particle mass. The zero-point energy is $6\hbar\omega$ and the zero-quantum ground state is nondegenerate. The one-quantum state has degeneracy $g_1=12$ and lies at energy $\hbar\omega$ above the ground state; the two-quantum level of $2\hbar\omega$ has degeneracy 78; the three-quantum state at $3\hbar\omega$ has degeneracy 364 and so on. Each of these totally symmetric IRs of U(12) contains states of various parity, angular momentum and permutational character, and part of our task is to sort out what these are.

We have applied the method of *inner plethysms*[10–14] to the classification of nonrigid limit states along the group chain

$$\mathrm{U}(12)\supset \mathrm{U}(4)\times\mathrm{U}(3)\supset S_5\times\mathrm{O}^I(3)\ . \tag{3}$$

This method, which provides branching rules for the reduction $\mathrm{U}(N-1)\downarrow S_N$ for *arbitrary* particle number N[10] has been discussed in detail by King,[13] Butler and King,[12] and Butler.[11] The use of generating function methods for the evaluation of plethysms is discussed in Ref. 14. $\mathrm{O}^I(3)$ is the external rotation-inversion group of all lab-fixed rotations and rotation inversions, and is a direct product

$$\mathrm{O}^I(3)=\mathrm{SO}^I(3)\times(E,E^*)\ , \tag{4}$$

where the inversion operator E^* inverts all particles through the molecular center of mass. Our results for $\nu\le 6$ quanta are presented in Table I, which gives the decomposition of five-body U(12) states $[\nu]$ according to parity $\pi=(-)^\nu$, angular momentum j and permutation symmetry. The IRs of the symmetric group S_5 are denoted by the partitions [5], [41], [32], [31^2], [2^21], [21^3], and [1^5] and have dimensions 1, 4, 5, 6, 5, 4, and 1, respectively. The character table for S_5 is given in, for example, Ref. 19, p. 265.

As well as considering homonuclear molecules containing five identical particles, we wish also to deal with the case where one of the particles is distinguishable from the rest, i.e., the (four + one)-body problem. The relevant group chain for the classification of the nonrigid limit states is here

$$\mathrm{U}(12)\supset \mathrm{U}(9)\times\mathrm{U}(3)\supset(S_4\times\mathrm{O}(3))\times\mathrm{O}(3)\supset S_4\times\mathrm{O}^I(3)\ . \tag{5}$$

The chain (5) shows that with one distinct particle the twelve originally identical oscillators split into two sets, containing nine and three oscillators, respectively. The classification of the (four + one)-body states (ν,ν'), where $\nu(\nu')$ is the number of quanta in U(9) (U(3)), according to parity, angular momentum and permutation symmetry is given in Table II. IRs of the symmetric group S_4 are denoted [4], [31], [2^2], [21^2], and [1^4], and are of dimension 1, 3, 2, 3, and 1. Note that the entries in Table II for $\nu'=0$ are identical with the results given previously for the reduction of four-body oscillator states along the chain[2]:

$$\mathrm{U}(9)\supset S_4\times\mathrm{O}^I(3)\ . \tag{6}$$

B. Rigid limit

We now define the idealized rigid limit. For the examples considered here, this is simply taken to be a conventional "rigid" molecule in which nuclei perform

small-amplitude vibrations about a well-defined equilibrium configuration that is itself undergoing overall rigid-body rotation. Coupling between rotations and vibrations is assumed negligible; in other words, rigid rotor quantum numbers are valid, and the rovibrational wave function can be written as a product of rotational and vibrational factors. Two further simplifying assumptions are made: First, that all vibrational modes in the molecule are degenerate and strictly harmonic; second, that the rigid rotor is a spherical top. While these assumptions result in artificially high imposed degeneracies for the rigid-limit states, there is no loss of generality since the idealized symmetry is readily broken. Thus, to obtain a particular realistic choice of rigid limit, we can easily allow normal modes to have different frequencies and be anharmonic, and substitute symmetric or asymmetric top levels for those of the spherical top. For the moment, however, we focus only on the essential features of the rigid/nonrigid correlation as revealed by use of the idealized rigid limit.

Let G be the point symmetry group of the rigid limit. Vibrational states are classified according to the group chain

$$U(3N-6)\supset G\ , \tag{7}$$

where $U(3N-6)$ is the unitary symmetry group associated with the degenerate set of normal modes. Rotational wave functions are classified according to the chain[20-22]

$$O(4)\overset{\text{iso}}{=}O^I(3)\times O^f(3)\supset O^I(3)\times G^f\ , \tag{8}$$

where $O^I(3)$ is the group of lab-fixed rotation inversions introduced earlier, $O^f(3)$ is the group of molecule-fixed rotation inversions, the direct product $O^I(3)\times O^f(3)$ is the "symmetry group of the spherical top"[20] [isomorphic with the four-dimensional rotation group O(4)], and G^f is a group of molecule-fixed transformations of rotational variables isomorphic with the point group G. Note that spherical top rotational wave functions span $(2j+1)^2$ dimensional IRs of the group $O^I(3)\times O^f(3)$. Electronic wave functions will be assumed totally symmetric throughout.

Independent of the strength of vibration/rotation coupling, the molecular Hamiltonian is formally invariant under the *complete nuclear permutation-inversion* (CNPI) group,[6] which is a subgroup of the kinematic symmetry group $S_N\times O^I(3)$:

$$\text{CNPI}\equiv S_N\times(E,E^*)\subset S_N\times O^I(3)\ . \tag{9}$$

As clarified through the work of Hougen,[23] Longuet-Higgins,[24] Bunker,[25] and others,[4,26] classification of a rigid molecule rotation–vibration-electronic (*rovibronic*) product wave function under its point symmetry group is equivalent to the classification of the nuclear spatial wave function with respect to the *permutation–inversion* (PI) or *molecular symmetry* (MS) group,[6] which is a subgroup (in general, proper) of the CNPI group consisting of all so-called *feasible* permutations and permutation inversions of nuclei. For nonlinear rigid molecules the PI group is isomorphic with the point group G itself (for linear molecules there is a homomorphism from the geometrical symmetry group $C_{\infty v}$ or $D_{\infty h}$ onto the PI group).

Contrary to the usual PI treatment of rotational wave functions, we wish to keep the molecular parity as a good quantum number even in the idealized rigid limit. This means that the rigid molecule wave functions must be classified in a subgroup of the nuclear permutation group S_N only, rather than the CNPI group, which in turn implies that rotational variables must be subjected to improper transformations when the point group G contains improper rotations. The transformation properties of rotational wave functions under improper rotations of axes are easily determined using the conventions introduced by Harter, Patterson, and da Paixio,[27] and by Berger.[22]

We therefore proceed as follows:

(i) Classify the rovibronic product wave functions in the rigid molecule symmetry group G and the group $O^I(3)$ (parity and total orbital angular momentum). For nonplanar rigid molecules, each rovibronic state is associated with a parity doublet.[28]

(ii) Using the relation between point group operations and permutations of nuclei, classify the rigid molecule rovibronic states in a subgroup G^τ of the nuclear permutation group S_N:

$$G^\tau\subset S_N\ . \tag{10}$$

(iii) The rigid molecule states must now be classified in the full permutation group S_N. This is accomplished using the group-theoretical method of *induction*.[29]

In the extreme rigid limit, each rovibronic state is associated (in addition to possible parity doubling) with a strictly degenerate set of $|S_N|/|G^\tau|$ states (where $|S_N|$ and $|G^\tau|$ are the orders of the groups of S_N and G^τ, respectively), corresponding to $|S_N|/|G^\tau|$ "localized vibrational domains" of the rigid molecule.[26] If the rovibronic state spans the IR Γ of G^τ with dimension $|\Gamma|$, the $|\Gamma|\cdot|S_N|/|G^\tau|$ dimensional representation of S_N spanned by the degenerate states is the *representation of S_N induced by the* IR Γ *of* G^τ, denoted[29]

$$\Gamma(G^\tau)\uparrow S_N\ . \tag{11}$$

Physically, induction from G^τ to S_N corresponds to delocalization of the wave function over all the localized vibrational domains. Mathematically, the S_N content of the induced representation $\Gamma(G^\tau)\uparrow S_N$ is determined using the *Frobenius reciprocity theorem*.[26,29] Thus, let Λ_i be an IR of S_N, and let the decomposition of Λ_i into IRs Γ_j of G^τ upon subduction to G^τ be

$$\Lambda_i\rightarrow\sum_j\Gamma_j C_{\Gamma_j,\Lambda_i}\ . \tag{12}$$

Then the Frobenius theorem states that the induced representation $\Gamma_j\uparrow S_N$ is

$$\Gamma_j\uparrow S_N=\sum\Lambda_i C_{\Lambda_i,\Gamma_j}\ , \tag{13a}$$

where the coefficient C_{Λ_i,Γ_j} of the IR Λ_i of S_N is

$$C_{\Lambda_i,\Gamma_j}=C_{\Gamma_j,\Lambda_i}\ , \tag{13b}$$

so that the content of the induced representation can be obtained via subduction (12).

Use of the method of induction therefore allows us to classify the rovibronic states of the rigid limit in the complete permutation group S_N. It should be noted that, as far as we shall be concerned, the only effect of nuclear spin is to determine the relative statistical weights of states spanning different IRs of S_N. Although nuclear statistical weights are not incorporated into the idealized correlation diagrams presented here, these factors can easily be taken into account if required.

Having outlined our general method for classification of rigid limit states in the kinematic symmetry group $S_N \times O^I(3)$, we turn to some particular examples.

1. Trigonal bipyramid

We consider first the trigonal bipyramidal configuration of the homonuclear X_5 rigid limit. The character table for the point group D_{3h} is given in Ref. 30, p. 566, and the correspondence between point group operations and elements of the permutation group S_5 is readily found. The permutations form a subgroup of S_5 of order 12, isomorphic with the group D_{3h}.

We can thereby obtain the D_{3h} content of IRs of S_5 appearing upon subduction to the D_{3h} subgroup. This information is presented in Table III. According to the Frobenius reciprocity relation described above, we obtain the representation of S_5 induced by a given IR of D_{3h} simply by reading down the appropriate column of Table III.

Classification of the $(2j+1)$ rotational states $|j,k\rangle$ (where $k=j, j-1, \ldots, -j$, the projection of the total angular momentum onto the molecule-fixed frame) under the point group D_{3h} is given in Ref. 30, p. 575 ($j \leq 4$). Each $|jk\rangle$ state is of course associated with $2j+1$ states $|jm\rangle$, corresponding to the different values of the external projection quantum number m. The vibrational modes of X_5 with symmetry D_{3h} span the IRs $2A_1' + 2E' + A_2'' + E''$. Recalling that we assume all these modes to be degenerate, the symmetry species corresponding to $v = 0, 1, 2, 3$ quanta of vibration are shown in Table IV. The total degeneracy of each vibrational state can be calculated using the formula (1) for U(9), appropriate for a nine-fold degenerate oscillator.

Using all the above information, we can classify the vibration–rotation states of idealized rigid D_{3h} with respect to the point group, and thence via induction in the complete kinematic group. In Table V positive parity rotation/vibration states are classified in $S_5 \times O^I(3)$ for $j \leq 4$, $v \leq 2$. For negative parity states, the contents of each row vector must be taken in reverse order.

TABLE III. Correlation of the IRs of the groups D_{3h} and S_5.

	A_1'	A_2'	E'	A_1''	A_2''	E''
[5]	1	0	0	0	0	0
[41]	1	0	1	0	1	0
[32]	1	0	1	0	0	1
$[31^2]$	0	1	1	0	1	1
$[2^21]$	0	0	1	1	0	1
$[21^3]$	0	1	0	1	0	1
$[1^5]$	0	0	0	1	0	0

TABLE IV. Classification of the vibrational states of $D_{3h}X_5$.

		A_1'	A_2'	E'	A_1''	A_2''	E''
v	g_v						
0	1	1	0	0	0	0	0
1	9	2	0	2	0	1	1
2	45	8	1	9	2	4	6
3	165	22	10	30	9	16	24

2. Tetrahedral

Another rigid limit of the homonuclear X_5 molecule that is of interest is the arrangement of four nuclei around a central particle in a configuration of tetrahedral symmetry. We proceed exactly as for the trigonal bipyramid. The character table for the point group T_d is shown in Ref. 2, as is the correspondence between point group operations and permutations of nuclei. The permutations form a subgroup of S_5 isomorphic with both the point group T_d and the symmetric group S_4, and the correlation table[6] for IRs of $T_d(S_4)$ and S_5 is given by the usual $S_N \downarrow S_{N-1}$ branching rules.[18]

Rotational wave functions are classified in T_d in, e.g., Ref. 30, p. 574, and the vibrational modes of tetrahedral X_5 span the IRs $A_1 + E + 2T_2$. Using the above results, it is straightforward to classify the rotation–vibration states of T_dX_5 in the group $O^I(3) \times S_5$.

Of interest as a basis for realistic treatment of methane-type molecules is the (four + one)-body rigid limit where the central atom is distinct from the others. The kinematic group here is $O^I(3) \times S_4$. This example is simpler than tetrahedral X_5, since a classification of the rotation–vibration states of XY_4 in the point group T_d is equivalent to classification in S_4, and there is no induction step involved.

3. Square pyramid

The correlation between the IRs of C_{4v}, which is the point group for square pyramidal X_5 and XY_4 molecules, and those of the groups S_5 (homonuclear X_5) and $S_4(XY_4)$ is shown in Tables VI and VII, respectively.

4. Pentagonal ring

We now consider the rigid limit where the five particles form a planar pentagonal ring having D_{5h} symmetry. The character table for the point group is given in Ref. 30, Table 51. Here we come across a feature not present in the previous examples. Thus, since the operation of reflection in the plane of the molecule is equivalent to the identity permutation of nuclei, there is a 2 : 1 correspondence (homomorphism) rather than a 1 : 1 correspondence (isomorphism) between elements of the point group D_{5h} and those of the group of distinct permutations of nuclei, which is of order 10 and isomorphic with D_5.

Although rotational[31] and vibrational states can separately be classified in the point group D_{5h}, the only "physical" rotation–vibration product states allowed are (assuming a totally symmetric electronic function)

TABLE V. Classification of vibration/rotation states of D_{3h} X_5 in the kinematic group $O^I(3)\times S_5$. Components of the row vectors give the number of IRs [5], [41], [32], [31^2], [2^21], [21^3], and [1^5] of S_5, respectively.

ν	$j=0+$	1+	2+	3+	4+
0	(1,1,1,0,0,0,0)	(0,0,1,2,1,2,0)	(1,2,3,2,2,1,0)	(0,2,2,4,3,3,1)	(1,4,4,4,4,2,1)
1	(2,5,5,4,3,1,0)	(1,7,10,14,12,11,3)	(5,17,20,22,18,13,3)	(4,19,25,32,27,23,6)	(8,29,35,40,33,25,6)
2	(8,21,23,20,17,9,2)	(7,39,52,70,58,51,13)	(23,81,98,110,92,69,17)	(22,99,127,160,133,111,28)	(38,141,173,200,167,129,32)

TABLE VI. Correlation of the IRs of the groups C_{4v} and S_5.

	A_1	A_2	B_1	B_2	E
[5]	1	0	0	0	0
[41]	1	0	0	1	1
[32]	1	0	1	1	1
[31^2]	0	1	0	1	2
[2^21]	1	1	1	0	1
[21^3]	0	1	1	0	1
[1^5]	0	0	1	0	0

TABLE VII. Correlation of the IRs of the groups C_{4v} and S_4.

	A_1	A_2	B_1	B_2	E
[4]	1	0	0	0	0
[31]	0	0	0	1	1
[2^2]	1	0	1	0	0
[21^2]	0	1	0	0	1
[1^4]	0	0	1	0	0

TABLE VIII. Correlation of the IRs of the groups D_5 and S_5.

	A_1	A_2	E_1	E_2
[5]	1	0	0	0
[41]	0	0	1	1
[32]	1	0	1	1
[31^2]	0	2	1	1
[2^21]	1	0	1	1
[21^3]	0	0	1	1
[1^5]	1	0	0	0

TABLE IX. Correlation of the IRs of the groups G_2 and S_5.

	A_1	A_2
[5]	1	0
[41]	2	2
[32]	3	2
[31^2]	2	4
[2^21]	3	2
[21^3]	2	2
[1^5]	1	0

those totally symmetric under reflection in the plane of the molecule, i.e., those having symmetry species with a single-dash superscript. In general, the homomorphism leads to the well-known result that rovibronic states of planar molecules have definite parities.[28]

The states of the rigid pentagonal ring are therefore classified according to groups:

$$O^I(3)\times D_{5h} \xrightarrow{ho} O^I(3)\times D_5 \uparrow O^I(3)\times S_5 \tag{14}$$

and the IRs of D_5 are correlated with those of S_5 in Table VIII.

5. Linear chain

The last rigid limit to be discussed here is the regular linear chain having $D_{\infty h}$ point symmetry. Since all rotations of the molecule about the linear axis are equivalent to the identity permutation of nuclei, there is an $\infty:1$ homomorphism from the point group onto the group of distinct feasible permutations of nuclei, denoted G_2. As is well known, this homomorphism leads to the introduction of the *extended* PI group for linear molecules.[32] The only allowed symmetry species in $D_{\infty h}$ for rovibronic states are $\sum_g^+$ and $\sum_u^{+\,27}$ and the states of the linear chain are classified as follows:

$$O^I(3)\times D_{\infty h} \xrightarrow{ho} O^I(3)\times G_2 \uparrow O^I(3)\times S_5\ . \tag{15}$$

IRs of the groups G_2 and S_5 are correlated in Table IX.

III. FIVE-BODY RIGID/NONRIGID ENERGY LEVEL CORRELATION DIAGRAM

Using the results obtained in the previous section, rigid/nonrigid energy level correlation diagrams can be constructed by invoking the noncrossing rule.

Correlation diagrams for X_5 rigid limits having tetrahedral (T_d), trigonal bipyramidal (D_{3h}) and square pyramidal (C_{4v}) symmetries are given in Figs. 1–3. All energy level scales shown are schematic. However, the ratio of the magnitude of the vibrational quantum in the nonrigid limit to that in the rigid limit is taken to be very roughly one half; this ratio is estimated by comparing the one-dimensional harmonic oscillator with the double minimum oscillator obtained from it by pushing up a barrier in the middle of the potential.[2] The (+) and (−) parity states of the nonplanar rigid limits are placed at opposite ends of the correlation diagrams for the sake of clarity. In the extreme rigid limit they are strictly degenerate.

The increasingly "vertical" nature of the rigid to nonrigid correlations as we proceed along the sequence T_d,

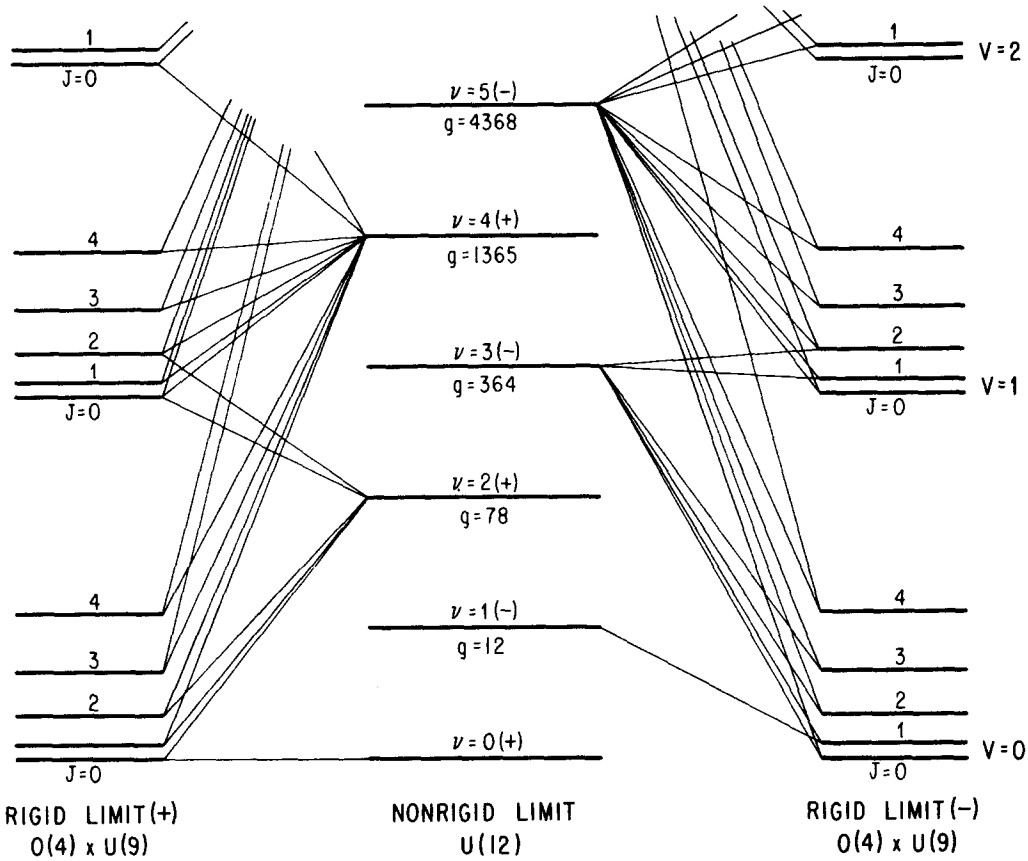

FIG. 1. Correlation diagram for five identical particles from the nonrigid to rigid tetrahedral (T_d) limits. The rigid limit manifold is split into two degenerate sets of states of opposite parity. The +(−) states connect to the even (odd) states in the nonrigid limit. Rigid limit states are labeled by the number of vibrational quanta v and the angular momentum J. The nonrigid limit states are labeled by the number of vibrational quanta v. Group designations at the bottom of the diagram indicate the symmetry appropriate for each region of the diagram.

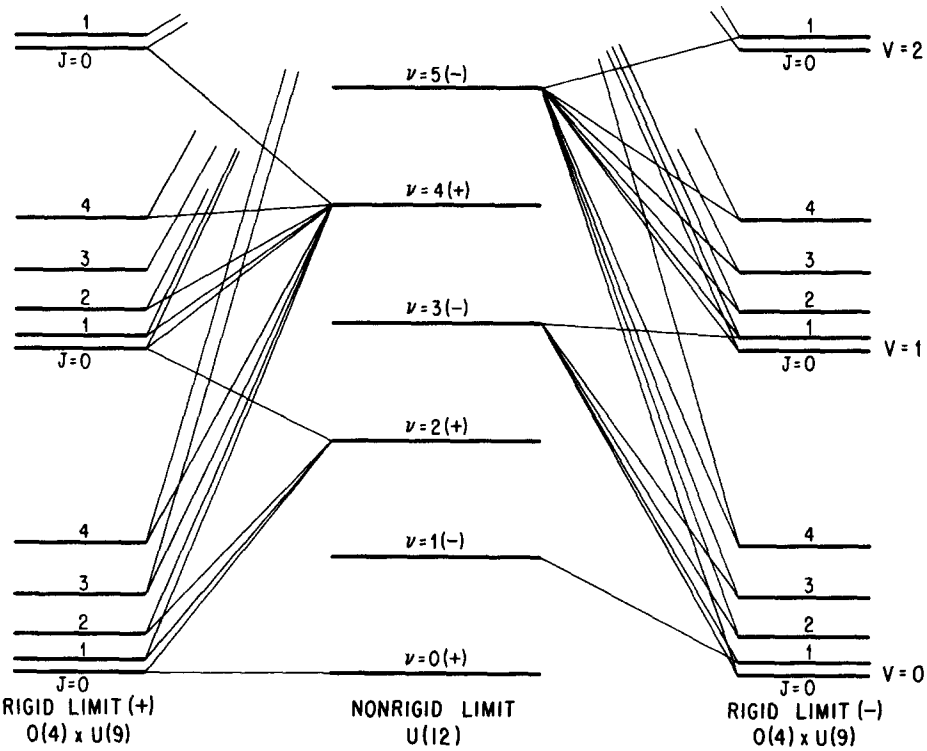

FIG. 2. Correlation diagram for five identical particles from the nonrigid to rigid trigonal-bipyramidal (D_{3h}) limits.

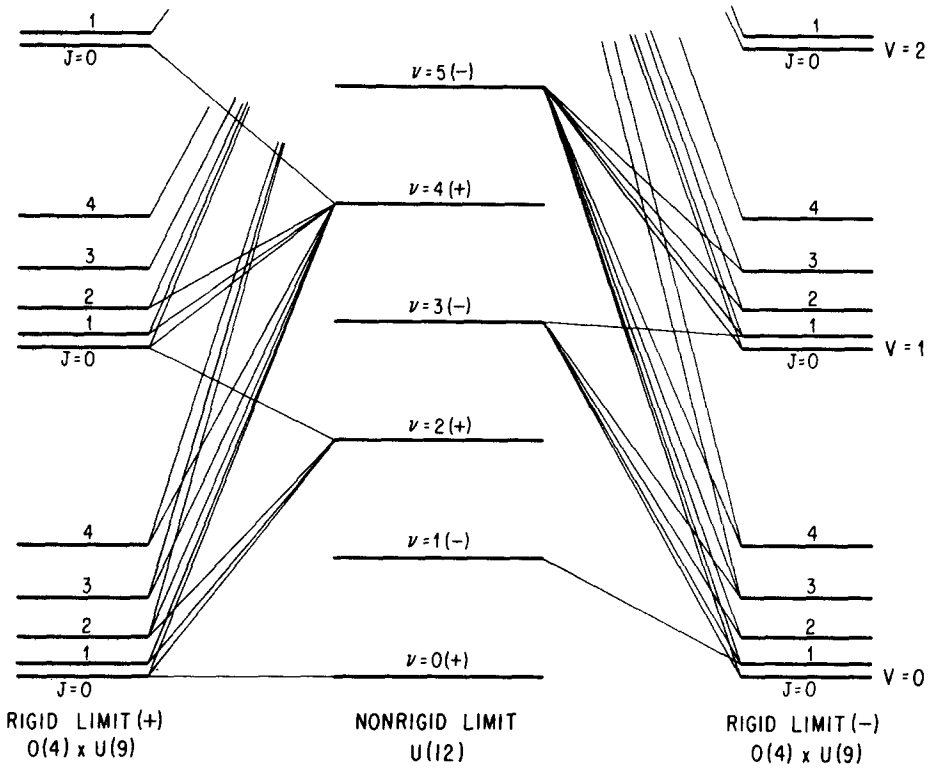

FIG. 3. Correlation diagram for five identical particles from the nonrigid to rigid square-pyramidal (C_{4v}) limits.

D_{3h}, and C_{4v} is due to the increasing clustering of rigid limit states (shown in our diagrams as degeneracy in the extreme rigid limit) as the order of the molecular point group decreases. This reflects the increased number of localized vibrational domains associated with lower symmetry structures. It is therefore harder to "melt" a cluster of low symmetry than one of high symmetry.

The correlation diagram for the planar X_5 ring (D_{5h}) is given in Fig. 4. In Fig. 5 we show a magnified portion of the diagram corresponding to the ground vibrational state rotational manifold of the rigid ring. The idealized spherical top symmetry of the rotational levels is broken to that of an oblate symmetric top, the individual k levels having parity $(-)^k$.

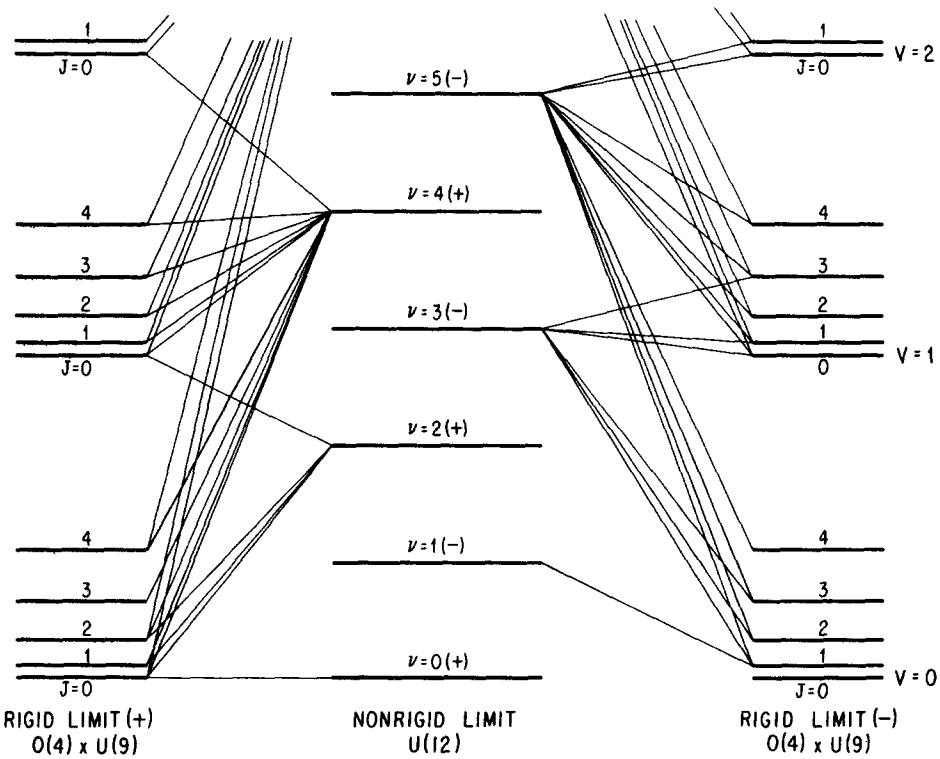

FIG. 4. Correlation diagram for five identical particles from the nonrigid to rigid pentagonal ring (D_{5h}) limits.

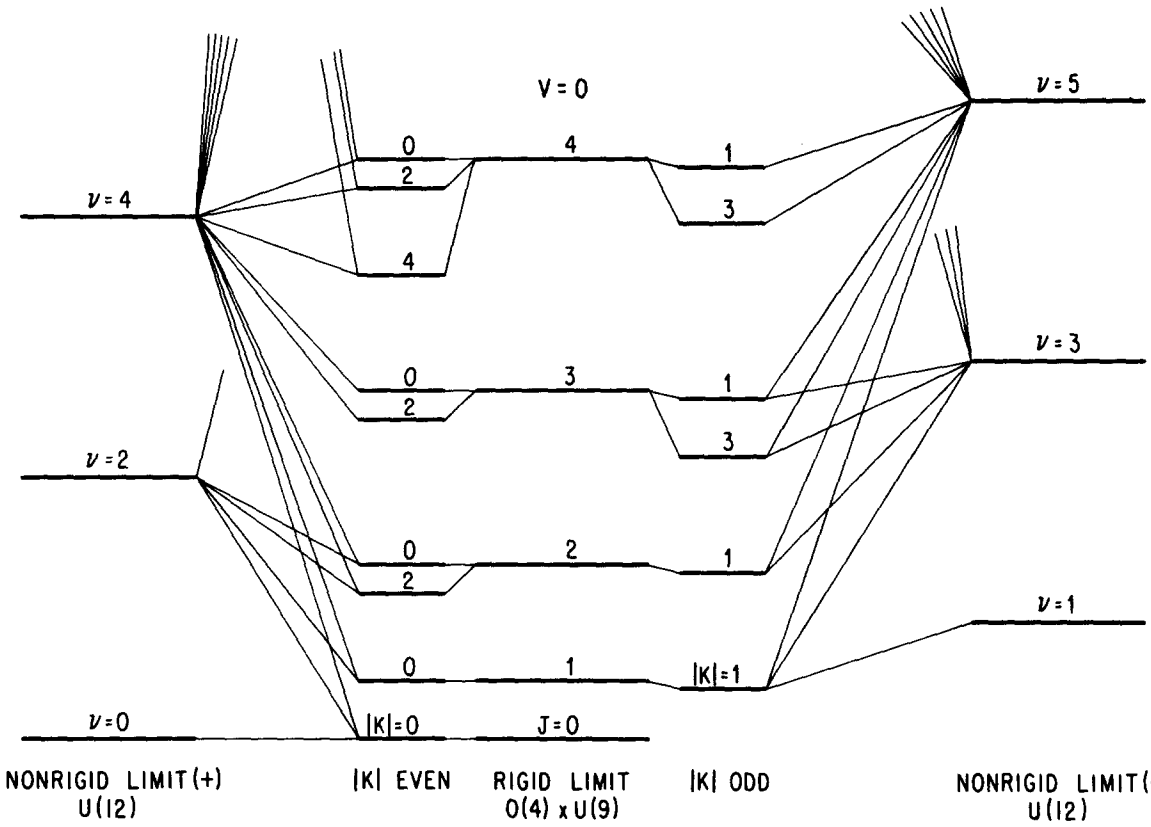

FIG. 5. Correlation diagram connecting the ground vibrational state of the rigid pentagonal ring to the nonrigid limit. The artificially high symmetry of the spherical top is removed in the rigid limit to give the energy level pattern of an oblate symmetric top. The parity of rigid limit states is given by $(-)^k$, where J and K are the rotational quantum numbers of the symmetric top.

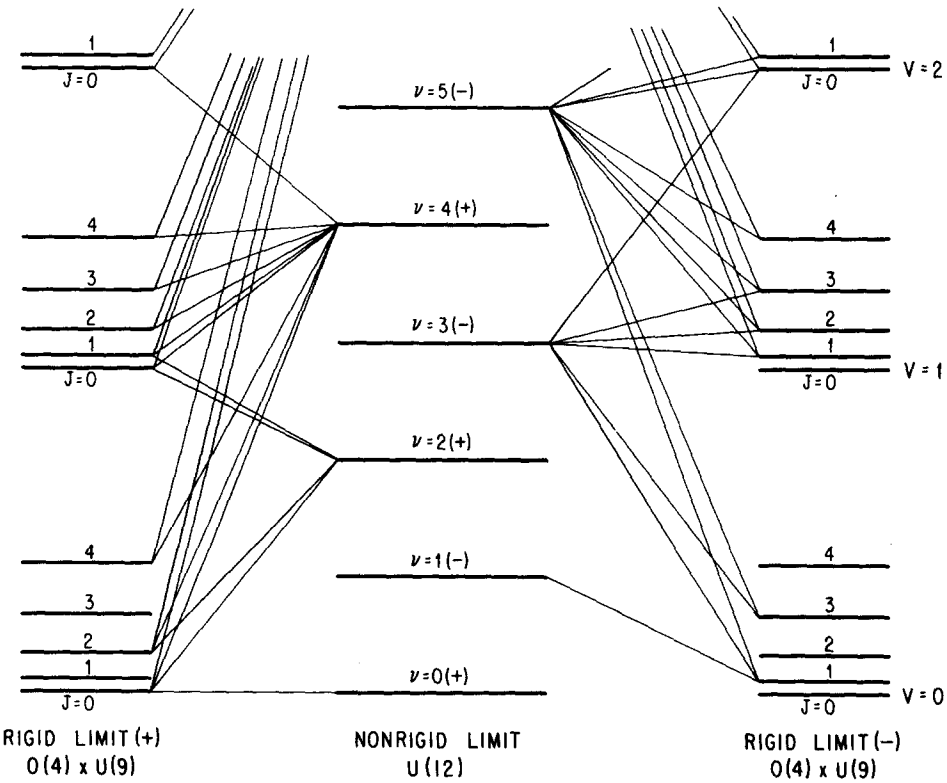

FIG. 6. Correlation diagram for five identical particles from the nonrigid to rigid linear ($D_{\infty h}$) limits.

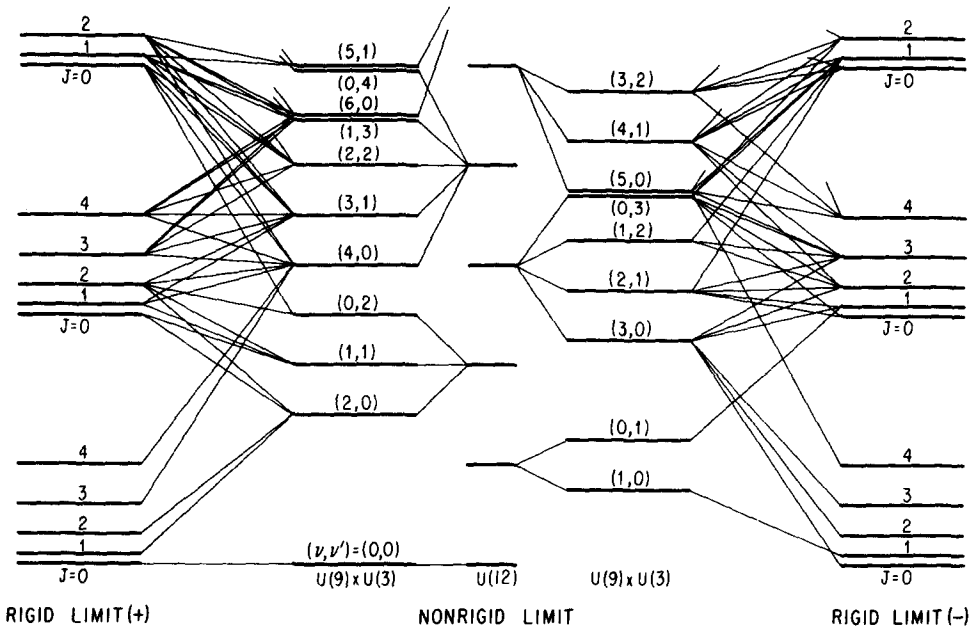

FIG. 7. Correlation diagram for (four + one)-particle system (XY_4) from the nonrigid to rigid tetrahedral (T_d) limits. The nonrigid limit states are labeled by two quantum numbers (ν, ν'), corresponding to the number of vibrational quanta in U(9) and U(3), respectively. The frequency ratio ω/ω' is taken to be 3/5.

The correlation diagram for the regular linear chain ($D_{\infty h}$) is shown in Fig. 6.

We next consider the case where one of the five nuclei in the molecule is different from the others. In Figs. 7 and 8 we present correlation diagrams for species XY_4 having rigid limit symmetries T_d and C_{4v}, respectively. In these diagrams the (four + one)-body nonrigid limit is characterized by two vibrational frequencies ω and ω', corresponding to the nine-dimensional (U(9)) and three-dimensional (U(3)) oscillators, respectively. The frequency ratio ω/ω' is taken to be 3/5 (cf. Sec. IV). Comparison with Figs. 1 and 3 shows that the XY_4 correlation diagrams exhibit relatively rich structure even before "deidealizing" the rigid and nonrigid limits (cf. Sec. V).

IV. (FIVE + ONE)-BODY PROBLEM

In this section we construct the rigid/nonrigid energy level correlation diagram for a (five + one)-body system that is of particular interest: that for which the rigid limit is a polyhedral molecule XY_5 having D_{3h} symmetry. This work represents a first step toward understanding energy level patterns in vibrationally excited states of molecules such as PF_5, where the experimentally well-established pseudorotation mode leads to complete scrambling of ligands on a relatively short time scale,[33] the hypothetical species PH_5, for which barriers to intramolecular H exchange are calculated to be extremely low,[34] and the fluxional ion CH_5^+.[35]

A. Nonrigid limit

States of the (five + one)-body nonrigid limit are clas-

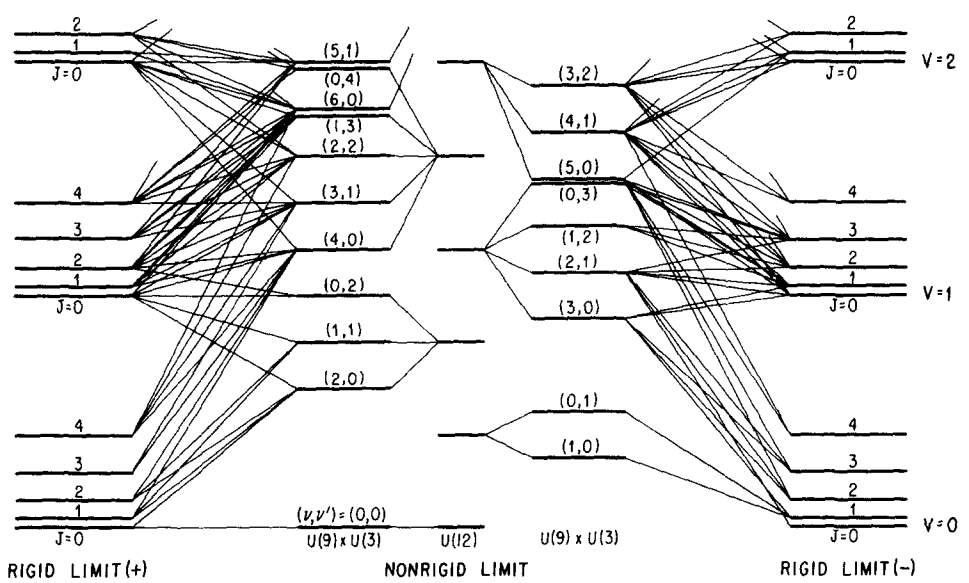

FIG. 8. Correlation diagram for (four + one)-particle system (XY_4) from the nonrigid to rigid square-pyramidal (C_{4v}) limits.

TABLE X. Classification of (five + one)-body nonrigid limit states according to their parity, angular momentum, and permutation symmetry.

$(\nu\ \nu')$	π	$j=$ 0	1	2
(0 0)	+	(1,0,0,0,0,0,0)		
(0 1)	−		(1,0,0,0,0,0,0)	
(1 0)	−		(0,1,0,0,0,0,0)	
(0 2)	+	(1,0,0,0,0,0,0)		(1,0,0,0,0,0,0)
(1 1)	+	(0,1,0,0,0,0,0)	(0,1,0,0,0,0,0)	(0,1,0,0,0,0,0)
(2 0)	+	(1,1,1,0,0,0,0)	(0,0,0,1,0,0,0)	(1,1,1,0,0,0,0)
(0 3)	−		(1,0,0,0,0,0,0)	
(1 2)	−		(0,2,0,0,0,0,0)	(0,1,0,0,0,0,0)
(2 1)	−	(0,0,0,1,0,0,0)	(2,2,2,1,0,0,0)	(1,1,1,1,0,0,0)
(3 0)	−	(0,0,0,0,0,1,0)	(1,3,2,2,1,0,0)	(0,1,1,1,1,0,0)
(0 4)	+	(1,0,0,0,0,0,0)		(1,0,0,0,0,0,0)
(1 3)	+	(0,1,0,0,0,0,0)	(0,1,0,0,0,0,0)	(0,2,0,0,0,0,0)
(2 2)	+	(2,2,2,0,0,0,0)	(1,1,1,2,0,0,0)	(3,3,3,1,0,0,0)
(3 1)	+	(1,3,2,2,1,0,0)	(1,4,3,3,2,1,0)	(2,6,4,4,2,0,0)
(4 0)	+	(3,4,4,1,2,0,0)	(0,2,2,4,2,2,0)	(3,6,6,4,3,1,0)
(0 5)	−		(1,0,0,0,0,0,0)	
(1 4)	−		(0,2,0,0,0,0,0)	(0,1,0,0,0,0,0)
(2 3)	−	(0,0,0,1,0,0,0)	(3,3,3,1,0,0,0)	(2,2,2,2,0,0,0)
(3 2)	−	(0,1,1,1,1,1,0)	(3,9,6,6,3,0,0)	(2,7,5,5,3,1,0)
(4 1)	−	(0,2,2,4,2,2,0)	(6,12,12,9,7,3,0)	(3,10,10,11,6,4,0)
(5 0)	−	(0,0,1,2,2,2,1)	(4,12,11,11,7,3,0)	(2,7,8,9,7,5,1)
(6 0)	+	(7,13,13,8,7,3,1)	(1,11,12,19,12,11,1)	(10,26,28,24,20,10,2)
(5 1)	+	(4,12,11,11,7,3,0)	(6,19,20,22,16,10,2)	(10,30,29,30,20,11,1)

$(\nu\ \nu')$	π	$j=$ 3	4	5	6
(0 0)	+				
(0 1)	−				
(1 0)	−				
(0 2)	+				
(1 1)	+				
(2 0)	+				
(0 3)	−	(1,0,0,0,0,0,0)			
(1 2)	−	(0,1,0,0,0,0,0)			
(2 1)	−	(1,1,1,0,0,0,0)			
(3 0)	−	(1,2,1,1,0,0,0)			
(0 4)	+		(1,0,0,0,0,0,0)		
(1 3)	+	(0,1,0,0,0,0,0)	(0,1,0,0,0,0,0)		
(2 2)	+	(1,1,1,1,0,0,0)	(1,1,1,0,0,0,0)		
(3 1)	+	(1,3,2,2,1,0,0)	(1,2,1,1,0,0,0)		
(4 0)	+	(0,2,2,3,1,1,0)	(2,3,2,1,1,0,0)		
(0 5)	−	(1,0,0,0,0,0,0)		(1,0,0,0,0,0,0)	
(1 4)	−	(0,2,0,0,0,0,0)	(0,1,0,0,0,0,0)	(0,1,0,0,0,0,0)	
(2 3)	−	(3,3,3,1,0,0,0)	(1,1,1,1,0,0,0)	(1,1,1,0,0,0,0)	
(3 2)	−	(3,8,5,5,2,0,0)	(1,3,2,2,1,0,0)	(1,2,1,1,0,0,0)	
(4 1)	−	(5,11,10,8,5,2,0)	(2,5,4,4,2,1,0)	(2,3,2,1,1,0,0)	
(5 0)	−	(4,11,10,10,6,3,0)	(1,4,4,4,3,2,0)	(2,4,3,3,1,0,0)	
(6 0)	+	(4,15,16,21,14,11,2)	(7,18,18,16,12,6,1)	(1,6,6,8,5,3,0)	(3,6,5,3,2,1,0)
(5 1)	+	(7,22,22,23,16,10,1)	(7,19,17,17,10,5,0)	(3,8,7,7,4,2,0)	(2,4,3,3,1,0,0)

sified along the group chain

$$U(15)\supset U(12)\times U(3)\supset (S_5\times O(3))\times O(3)\supset S_5\times O^I(3)\ . \qquad (16)$$

Decomposition of the states (ν, ν'), where $\nu(\nu')$ is the number of quanta in U(12) (U(3)), according to parity, angular momentum, and permutation symmetry is given in Table X. The entries in this table for $\nu'=0$ are identical with the results given in Table I for the reduction of five-body oscillator states along the chain

$$U(12)\supset S_5\times O^I(3)\ .$$

The (five + one)-body nonrigid limit is characterized by two energy spacings $\hbar\omega$ and $\hbar\omega'$, corresponding to 12-dimensional and 3-dimensional oscillators, respectively. The ratio ω/ω' is here taken to be 3/5, which represents a very rough estimate of the force constants appropriate for a highly nonrigid PF_5 molecule. The resulting sequence of energy levels should however only be regarded as schematic.

B. Rigid limit

Applying the methods used for the five-body problem, classification of the rotation–vibration states of the

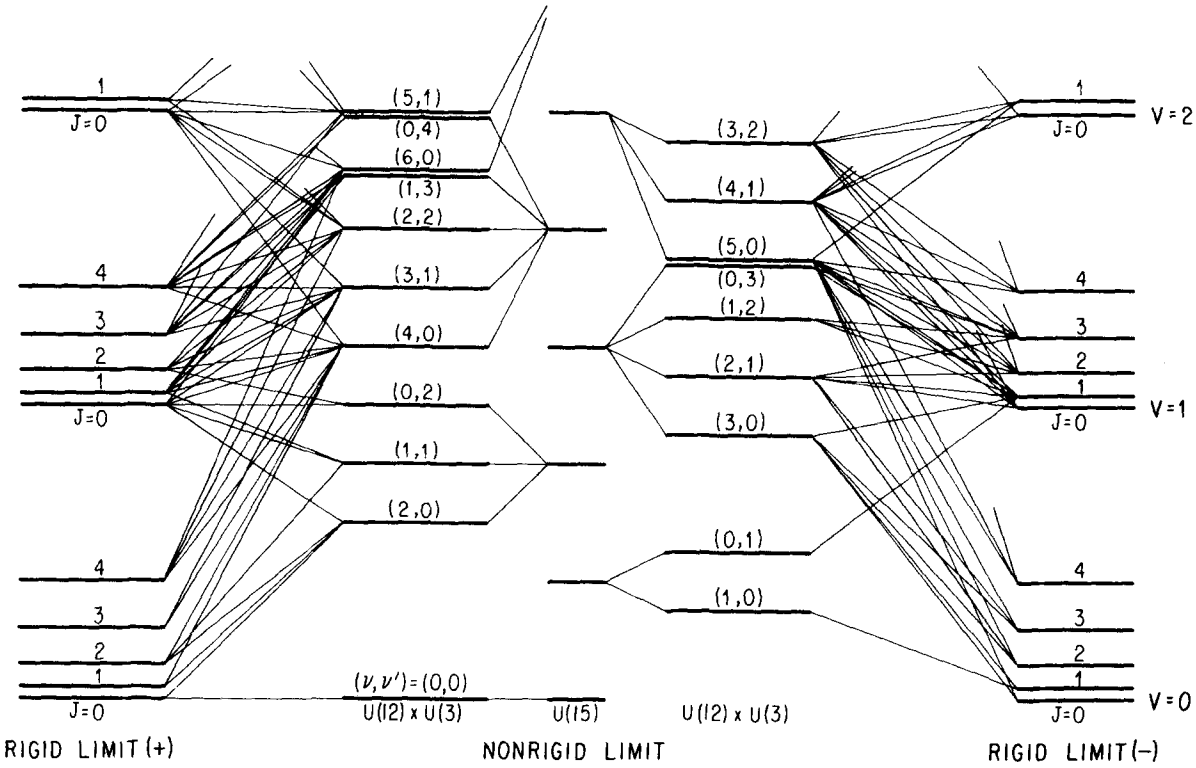

FIG. 9. Correlation diagram for (five+one)-particle system (XY_5) from the nonrigid to rigid trigonal-bipyramidal (D_{3h}) limits. The nonrigid limit states are labeled by two quantum numbers (ν,ν'), corresponding to the number of vibrational quanta in U(12) and U(3), respectively. The frequency ratio ω/ω' is taken to be 3/5.

idealized D_{3h} XY_5 rigid limit in the groups

$$O^I(3)\times D_{3h} \downarrow O^I(3)\times S_5$$

is quite straightforward. The rigid/nonrigid energy level correlation diagram is shown in Fig. 9.

V. CONCLUSION

In this work we have constructed rigid/nonrigid energy level correlation diagrams for several five- and six-body systems. Our treatment of polyhedral XY_4 and XY_5 model systems has brought us close to a point where we can use the correlation diagrams as a means for understanding energy level patterns for excited vibration–rotation states of real molecules. Let us now consider what remains to be done before this is possible

First of all, the idealized rigid limit has to be made more realistic by breaking the artificially high imposed symmetry. Thus, instead of an idealized level pattern corresponding to a spherical top rotor with $(3N-3)$-fold degenerate vibrational states, the rigid limit must be correlated to a realistic zeroth-order vibration–rotation manifold calculated from molecular parameters determined in the ground and lowest excited vibrational states. Procedures for this step are well known; with adequate molecular data, this stage poses no problem.

Second, the high degeneracy of the nonrigid limit should be broken to reflect more realistic pair interactions than pure harmonic. In particular, the effects of hard-core repulsions should be taken into account to break the $U(3N-3)$ symmetry. Insofar as the energy changes associated with the cores are small relative to the energy level spacing in the ideal nonrigid limit, the broken $U(3N-3)$ will still retain a semblance of shell structure reflecting the $U(3N-3)$ parentage, i.e., perturbation theory will apply.

The deidealized limits can then be connected to give a more realistic rigid/nonrigid correlation diagram.

Finally, it must be realized that each connecting line in the present idealized correlation diagrams corresponds in general to a *set* of energy levels. Although the levels in each set are shown as degenerate for the sake of clarity, in reality they are necessarily split. In effect, the idealized degenerate sets of our diagrams will behave as "parent sets" for groups of states in a manner analogous to the role of atomic states in crystal field theory, or localized molecular rovibronic states in Dalton's approach. It may be that the introduction of realistic hard-core repulsions in the nonrigid limit will completely remove the apparent clustering of levels; however, it would not be surprising if some near degeneracy or clustering remains.[27] Then, if the physical picture we have developed has any validity, by suitable averaging over bunches of energy levels it should be possible to place a given system at a particular point along the correlation diagram. We can then expect to begin to use the diagrams to interpret rotation/vibration spectra of highly nonrigid molecules, e.g., those whose moments of inertia vary significantly from one vibrational level to another.

ACKNOWLEDGMENTS

G. S. E. would like to thank the U. K. Science Research Council for the award of a NATO Postdoctoral Research Fellowship. We would both like to acknowledge the hospitality of the Laboratoire de Photophysique Moléculaire, Université de Paris-Sud, Orsay, France, where much of this research was done. The work was supported in part by a Grant from the National Science Foundation.

[1]M. E. Kellman and R. S. Berry, Chem. Phys. Lett. **42**, 327 (1976).
[2]F. Amar, M. E. Kellman, and R. S. Berry, J. Chem. Phys. **70**, 1973 (1979).
[3]F. Amar, M. E. Kellman, and R. S. Berry, J. Chem. Phys. **73**, 2387 (1980).
[4]B. J. Dalton, Mol. Phys. **11**, 265 (1966).
[5]B. J. Dalton, J. Chem. Phys. **54**, 4745 (1971).
[6]P. R. Bunker, *Molecular Symmetry and Spectroscopy* (Academic, New York, 1979),
[7]G. A. Natanson, Abstracts of Fourteenth Annual Midwest Theoretical Chemistry Conference, Chicago, 1981 (unpublished work).
[8]A. R. W. McKellar and H. L. Welsh, Can. J. Phys. **52**, 1082 (1974); R. G. Gordon and J. K. Cashion, J. Chem. Phys. **44**, 1190 (1966); P. R. Bunker, Can. J. Phys. **57**, 2099 (1979).
[9]Ch. J. Bordé, M. Ouhayoun, A. van Leberghe, C. Salomon, S. Avrillier, C. D. Cantrell, and J. Bordé, in *Laser Spectroscopy IV*, edited by H. Walther and K. W. Rothe (Springer, New York, 1979).
[10]F. D. Murnaghan, Proc. Natl. Acad. Sci. (USA) **41**, 514, 1096 (1955).
[11]P. R. Butler, J. Phys. (Paris) **C4**, **31**, 4 (1970).
[12]P. R. Butler and R. C. King, J. Math. Phys. **14**, 1176 (1973).
[13]R. C. King, J. Math. Phys. **15**, 258 (1974).
[14]J. Patera and R. T. Sharp, J. Phys. A **13**, 397 (1980).
[15]S. Gartenhaus and C. Schwartz, Phys. Rev. **108**, 482 (1957).
[16]P. Kramer and M. Moshinsky, in *Group Theory and its Applications*, edited by E. M. Loebl (Academic, New York, 1968), Vol. 1.
[17]G. A. Baker, Phys. Rev. **103**, 1119 (1956).
[18]M. Hamermesh, *Group Theory* (Addison-Wesley, New York, 1962).
[19]D. E. Littlewood, *The Theory of Group Characters* (Oxford, Clarendon, 1950).
[20]J. D. Louck and H. W. Galbraith, Rev. Mod. Phys. **48**, 69 (1976).
[21]J-C. Hilico, H. Berger, and M. Loete, Can. J. Phys. **54**, 1702 (1976).
[22]H. Berger, J. Phys. (Paris) **38**, 1371 (1977).
[23]J. T. Hougen, J. Chem. Phys. **37**, 1433 (1962); **39**, 358 (1963).
[24]H. C. Longuet-Higgins, Mol. Phys. **6**, 445 (1963).
[25]P. R. Bunker, in *Vibrational Spectroscopy and Structure*, edited by J. R. Durig (Marcell Dekker, New York, 1975), Vol. 3.
[26]J. K. G. Watson, Can. J. Phys. **43**, 1996 (1965).
[27]W. G. Harter, C. W. Patterson, and F. J. da Paixao, Rev. Mod. Phys. **50**, 37 (1978).
[28]T. Oka, J. Mol. Spec. **48**, 503 (1973).
[29]S. L. Altmann, *Induced Representations in Crystals and Molecules* (Academic, New York, 1977).
[30]G. Herzberg, *Electronic Spectra and Electronic Structure* (Van Nostrand, New York, 1966).
[31]A. Weber, J. Chem. Phys. **73**, 3952 (1980).
[32]P. R. Bunker and D. Papoušek, J. Mol. Spec. **32**, 419 (1969).
[33]G. M. Whitesides and H. L. Mitchell, J. Am. Chem. Soc. **91**, 5384 (1969).
[34]W. Kutzelnigg, in *Proceedings of the Conference on Molecular Structure, Rigidity and Potential Energy Surfaces*, Bielefeld, 1980, edited by J. Hinze (Plenum, to be published).
[35]M. F. Guest, J. N. Murrell, and J. B. Pedley, Mol. Phys. **20**, 81 (1971).